Carbon nanotube bundles under high pressure: Transformation to low-symmetry structures

Siu-Pang Chan,[1] Wai-Leung Yim,[1] X. G. Gong,[1,2,3,*] and Zhi-Feng Liu[1,*]

[1]*Department of Chemistry, The Chinese University of Hong Kong, Shatin, Hong Kong, China*

[2]*Institute of Solid State Physics, Chinese Academy of Sciences, Hefei, Anhui, China*

[3]*Department of Physics, Fudan University, Shanghai, China*

Structure transformations for crystalline bundles of single walled carbon nanotubes (10,10), (8,8), and (6,6), in response to external pressure are modeled by first-principles calculations. Upon pressure, the circular tube section is first transformed into an elliptical shape. Further pressure then leads to a flattened shape, similar to a 400-m track, with two flat sections connected by two cap sections. While the stress is taken up at the cap sections by bond buckling, the conjugate π bonding on the two flat sections becomes more effective and provides some stabilization for the structure. Such a transformation effectively squeezes the empty space inside a tube and thus reduces the intertube van der Waals repulsion. Collapse of the tube structures or linking between tubes via sp^3 bonding is not observed up to a stress level of 20 GPa. Hexagonal tube sections are also observed, which is a metastable state, due to the the symmetry constraint of the triangular lattice during structure optimization. Such a structure is not favored as it is too rigid to adapt to external pressures.

I. INTRODUCTION

One of the most extensively studied properties of carbon nanotubes (CN's) is their elastic response to external forces, due to the general interests in their mechanical properties and in their potential application as ultrastrong materials.[1,2] Along the axial direction, carbon nanotubes are highly stiff with a Young's moduli in the terapascal range.[3] However, along the radial direction, carbon nanotubes are extraordinarily flexible and elastic. Their circular sections can be deformed, and even collapsed,[4,5] as induced by external forces,[6] local bents or defects,[7] or by van der Waals forces.[8]

The elasticity of a CN bundle is especially interesting. Such bundles are composed of more than hundreds of aligned tubes. In a crystalline bundle, often used in theoretical modeling, the tubes are idealized as having a uniform tube diameter in a two-dimensional triangular lattice,[9] although in experiments the tube diameter may fall into a narrow range of values. CN based fibers are expected to come in this form, which can now be made in small quantities.[10–12] With the symmetry constraint of the two-dimensional triangular lattice, the section of an individual CN should be deformed into honeycomb hexagonal structure upon the exertion of external pressure, according to elastic models,[13,14] and such transformations could have significant implications for the electronic and vibrational properties of CN's.

A number of experimental studies on the pressure induced structural transformation have been reported, which generally fall into two categories in terms of experimental technique. The first is based on Raman spectra.[15–17] Structure transformation is indicated by the disappearance of the symmetric radial breathing modes[18–20] between 150 and 200 cm^{-1}, which is attributed to the loss of electronic resonance in the Raman scattering as the structure is transformed under pressure. The other technique used is diffraction, by either x ray[21,22] or neutron.[23] In such experiments, the structural change is measured directly as pressure is varied. However, the inconsistency in the results from different groups, prob-

ably due to sample preparation and also to poor resolution, is yet to be resolved.[21–23]

There are strong evidences from both Raman[16,17] and diffraction[21,23] experiments indicating a phase transition around the pressure of 1–2 GPa. However, the exact nature of this transition is controversial. Based on generalized tight-binding molecular-dynamics calculation, Venkateswaran *et al.*[16] attributed the transition to the distortion of the circular cross section of the tubes into hexagonal shape, in agreement with elastic models.[13,14] On the other hand, using empirical force fields, Peters *et al.*[17] assigned this transition to a change of the circular cross section into an ellipse. Very recently, Sluiter *et al.* have studied the (10,10) and (12,12) bundles, using an *ab initio* method based on density-functional theory (DFT).[24] Upon pressure, they found a hexagonal cross section for the (12,12) tube, but an elliptical cross section for the (10,10) tube. This difference is attributed to the fact that bundles of (12,12) tubes are commensurate with the symmetry of the triangular lattice.

It is well known that the conjugate π bonding among carbon atoms plays a significant role in stabilizing a flat graphene sheet. As the cross section of the tube changes into a hexagonal shape, each of the six sides becomes more like a flat graphene sheet, with more effective conjugate π interactions. Such an effect is compensated by the bond angle distortion around the hexagonal corners and the van der Waals repulsion among the neighboring tubes. With the development of *ab initio* methods for molecular modeling, it is now possible to give a good account of all these factors from first principles.

We hereby report a computational study on the bundles of (6,6), (8,8), and (10,10) tubes under high pressure, using the DFT method with pseudopotentials and a plane-wave basis set. Our results show that for such bundles, the structure with hexagonal cross section is metastable under high pressure due to its stiffness enforced by its high symmetry. In the real stable structure, the tube sections are deformed to a flattened shape similar to a 400-m track, with two flat graphene sec-
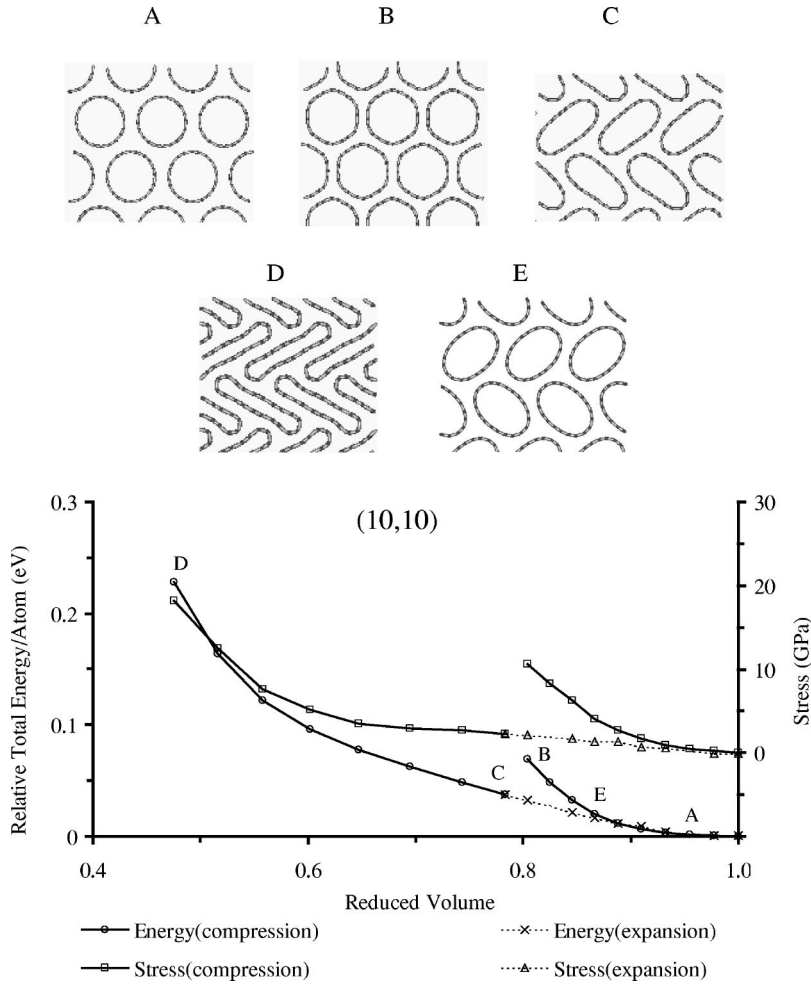
FIG. 1. The total energy/atom relative to that at $RV=1.0$ and lattice stress in the a direction for a crystalline bundle of (10,10) carbon nanotubes is plotted as a function of the reduced volume. The shapes of the tube sections for selected points on the curves are also shown as insertions. Along the compression curve, the circular structure A is transformed into a hexagonal structure B, as RV decreases. The flattened structure C, with two flat graphene sections connected by two curved caps, is found upon further compression, with a sudden drop in energy. B is actually a metastable structure, due to the symmetry constraint of the lattice. A continuous curve is recovered in the expansion curve, which crosses with the compression curve at point E. Under increasing pressure, the tube sections change first from circular (A) to elliptical (E) and finally to flattened shape (C and D).

tions connected by two curved caps. The stress at high pressure is mainly taken up locally in the cap sections by extensive bond buckling. Such a structural response, due to the interplay among van der Waals repulsion, conjugate π bonding on the flat sections, and bond buckling on the caps, underlies the extraordinary compressibility of carbon nanotube bundles.

II. COMPUTATIONAL DETAILS

Our DFT calculations are performed with a plane-wave basis set,[25,26] Vanderbilt ultrasoft pseudopotentials for the atomic core regions,[27,28] and the exchange-correlation functional within the generalized gradient approximation (GGA),[29] as implemented in the Vienna Ab-Initio Simulation Package (VASP).[30–32] For structure optimization, the cutoff energy is 287 eV for the plane-wave basis set, and two k points are used in the average sampling. For the calculation of lattice stress, the cutoff energy is raised to 380 eV.

A crystalline bundle of single walled CN's are modeled by a rectangular unit cell containing two tubes. The length of c is at 4.996 Å in accordance with the periodicity along the tube axis. It is fixed in all calculations, which will certainly introduce some inaccuracy. However, the error is expected to be small as it is well understood that carbon nanotubes are highly stiff along the axial direction.[3] The lengths of a and b

are held at fixed proportion to enforce two-dimensional triangular tight packing, while external pressure is introduced in the a and b directions by decreasing the length of a, together with a proportional decrease for b. The stress along the a and b directions are thus approximately equal to each other. A similar setup has been used before in the study of H_2 interaction with CN bundles under high pressure.[33]

III. RESULTS

Shown in Fig. 1 are the calculated energy and lattice stress for a crystalline bundle of (10,10) tubes as a function of the reduced volume of the unit cell. The reference volume is obtained by minimizing the total energy versus both the tube structure and the lattice parameters a. For the (10,10) tubes, the energy minimum is found at $a=17.4$ Å, which is in good agreement with previous DFT calculations, and as expected, larger than the value of 16.5 Å obtained by local density-functional method.[24] At this point, the unit-cell volume is taken as $RV=1.0$, and the energy for the optimized structure is at a minimum, with the tube being circular (A). As RV is reduced stepwise from 1.0, pressure is introduced on the unit cell, and at each step structure optimization is performed so that the force on each carbon atom is less than 0.02 eV/Å. The initial geometry for the tubes are taken from the optimized structure at the previous (and thus slightly

larger) RV. These steps produce the "compression" curve shown in Fig. 1.

The energy increases along the compression curve as RV decreases. The tube structure remains circular until at the point of $RV=0.8$, when the tube section becomes hexagonal, as in B. The lattice stress, which could be taken approximately as the value of external pressure, increases to 10.6 GPa. However, at the next step $RV=0.78$, the tube section goes through dramatic changes during structure optimization and becomes flattened. This newly identified structure C is distinct from the previously suggested hexagonal or elliptical sections, and has a shape similar to a 400-m track, with two flat sections connected by two caps. Moreover, there is a drop of 5.1 eV (0.032 eV/atom) in the total energy, while the calculated stress shows an even more dramatic drop from 10.6 GPa for the hexagonal B to 2.3 GPa for the flattened C, even though the unit cell is slightly reduced.

Starting with C ($a=15.4$ Å), the previous procedure is repeated, albeit with RV increased stepwise, to produce a set of points in Fig. 1 labeled as the "expansion" curve. Along this curve, the structure gradually changes from the flattened C into the elliptical E. In terms of energy, the point on the expansion curve is considerably lower than that for the corresponding point on the compression curve with the same RV. However, at $RV=0.89$, the expansion curve crosses the compression curve, and for $RV>0.89$, the energy ordering is reversed with the compression curve below the expansion curve, although the energy difference is not as large as in the region of $0.80<RV<0.89$. The optimized structure on the expansion curve remains elliptical from $RV=0.89$ all the way up to $RV=1.0$, although its shape is gradually approaching a circle.

Comparison between these two curves indicates that the hexagonal B, together with other points on the compression curve in the region of $0.78<RV<0.89$, are actually metastable, as the symmetry constraint in the two-dimensional triangular lattice leads our structure optimization to a local minimum with higher energy. The stable structure in this region is either flattened (C) or elliptical (E). In contrast, in the region of $0.89<RV<1.0$, the elliptical structures on the expansion curve are metastable, while the stable structures have circular sections as those on the compression curve.

Based on these results, the (10,10) tube should be circular in the real compression experiment, up to $VR=0.89$. A structure transition from a circular to elliptical section should occur around $VR=0.89$, facilitated by thermal motion of carbon atoms to break the symmetry constraint of the triangular lattice. At this point, the pressure obtained on the compression curve is 2.7 GPa, while on the expansion curve the pressure is 1.4 GPa, which can be compared with the experimentally observed structural transition in bundles of (10,10) tubes at 1.5–1.7 GPa, previously identified by changes in Raman spectra.[16,17] The *ab initio* results thus support the interpretation of this transition as from a circular to an elliptical section,[17] rather than to a hexagonal section.[16]

Upon further compression, the elliptical structure E is deformed into structure C. An ellipse shape becomes untenable at higher pressure as a flattened ellipse would produce two sharp corners, which must be built upon an extraordinary degree of bond buckling. This problem is alleviated in structures C and D by the presence of the two cap sections. In addition, each flat section in C and D could be viewed as a graphene sheet, and conjugate π bonding among carbon atoms is more effective on such a flat section than that on an elliptically curved section. Moreover, the surfaces of the graphene sections in C and D are slightly deformed due to intertube interactions in the periodic two-dimensional lattice. The symmetry of the tube is thus lowered due to strong intertube repulsion, which is a marked deviation from the highly symmetric circular, hexagonal, and elliptical structures.

For the bundles of (6,6) and (8,8) tubes, the general trend is similar to the bundle of (10,10) tubes, as shown in Fig. 2. The energy minimum at $RV=1.0$ corresponds to $a=15.0$ Å for the (8,8) bundle, and to $a=12.0$ Å for the (6,6) bundle. Along the compression curve, structure optimization again leads to metastable structures, with high symmetry circular or hexagonal section. At $RV=0.73$ for both the (8,8) and (6,6) bundles, a fall in total energy is observed, together with a dramatic fall in lattice stress, as the tube section is transformed into a flattened shape during structure optimization. The fall in energy is less for the (6,6) and (8,8) tubes than that for the (10,10) tubes, while the fall in stress is comparable in magnitude.

At the same RV value (say, $RV=0.7$), the lattice stress increases when the tube diameter decreases, as shown by comparing the results shown in Figs. 1 and 2 for the (10,10), (8,8), and (6,6) tubes. Also, the increase in lattice stress is faster for tubes with smaller diameters, indicating that the smaller the tube diameter, the harder to compress it. Shown in Fig. 3 are the flattened tube structures at a pressure around 13 GPa. The (8,8) and (10,10) tubes are similar to each other, except that the flat sections in the (10,10) tube is longer. On the hand, the section for the (6,6) tube is more elliptical, probably due to its small diameter.

IV. DISCUSSIONS

A. Hexagonal versus flattened sections

It should be noted that based on the elastic model, the tube section would spontaneously changes into the hexagonal shape for a bundle of tubes with diameters over 25 Å.[13] Experimentally, polygonization of the tube section was observed around 17 Å, without any external pressure.[34] The often cited reason for such a change is the attractive intertube van der Waals interaction in the triangular lattice as the tubes are flattened with six sides.[13] There is one additional reason for the preference of such a structure. Each flat section could also be seen as a graphene sheet on which the conjugate π bonding is more effective than that on a circular surface, further stabilizing the structure. On the other hand, the formation of a hexagonal section produces six localized corners with bond buckling, which raises the total energy. Both the attractive van der Waals interaction and the conjugate π bonding on the flatten sections increase as the tube diameter increases. Thus for a bundle of tubes with large diameters, hexagonal shape is favored.
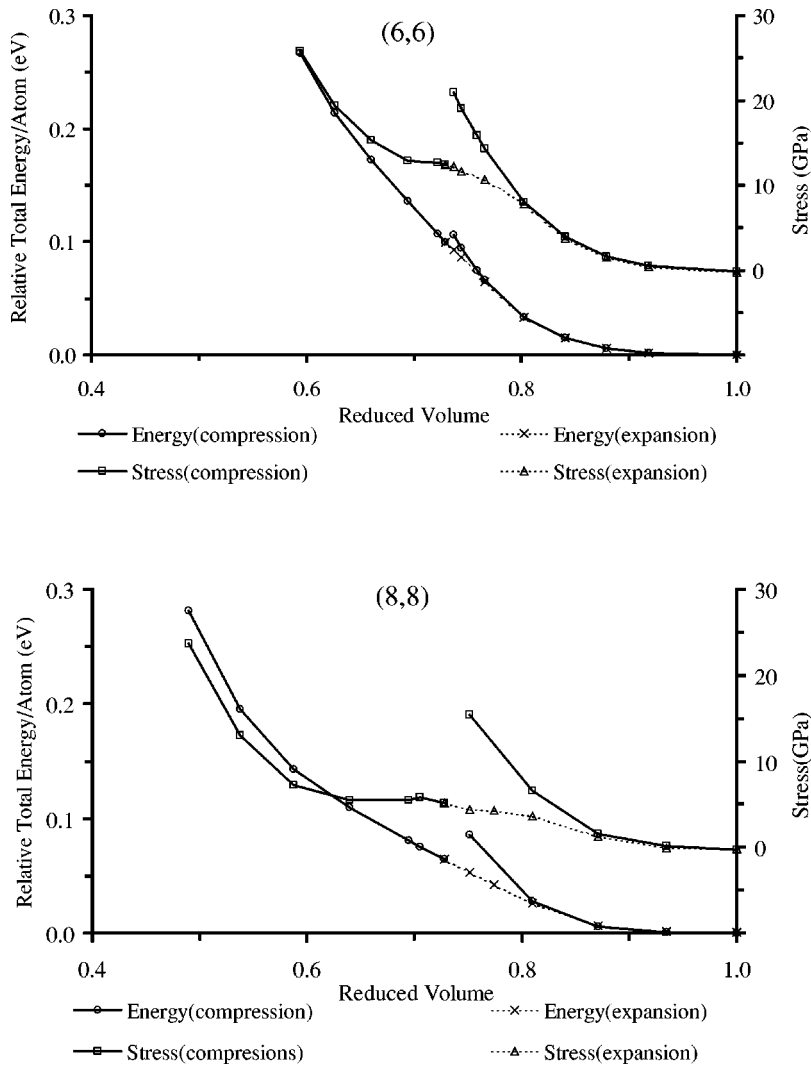
FIG. 2. The total energy/atom relative to that at $RV = 1.0$ and lattice stress in the a direction for a crystalline bundle of (6,6) or (8,8) carbon nanotubes is plotted as a function of the reduced volume.

However, upon compression, intertube van der Waals interaction becomes a serious disadvantage in terms of energy, as it enters the regime of steep repulsion. To reduce such repulsion, the preferred structure must be flexible and compressible. In such a situation, the flattened structure C has distinct advantages over the hexagonal structure B which is fairly rigid due to its high symmetry.

Structural compression on the carbon nanotubes could be achieved in two ways, either by contraction of C-C bonds, or by bond angle buckling. Among these two, bond contraction is considerably stiffer than bending bond angles.[20] At $RV = 1.0$, the calculated C-C bond distance in the circular A is 1.42 Å for C-C bonds perpendicular to the direction of the tube (labeled as C-$C_\perp$) and 1.44 Å for others (labeled as C-C_{ℓ}). The difference is due to the fact that we fix the axial lattice parameter in our calculations. These values are compared favorably with the 1.42-Å C-C bond distance in graphite. Although significant deformation is observed in structure C, the average bond distance remains around 1.42 Å for C-$C_\perp$ and 1.44 Å for C-C_{ℓ}, as in A. This is in sharp contrast to the hexagonal B, for which the average bond distance for C-$C_\perp$ is significantly shortened to $\sim$1.39 Å while the C-C_{ℓ} distance is also shortened to $\sim$1.42 Å.

Such differences can be explained by the symmetry constraint. For B, buckling is distributed on six corners and its extent is basically fixed in order to maintain the hexagonal symmetry. When further pressure is applied, the hexagonal B could only respond by the contraction of C-C bonds, which makes it energetically costly to compress the tubes. In contrast, bond buckling for the low-symmetry flattened structure (C and D) is localized on the two cap sections and could go to a much larger extent to squeeze the space inside the tube, without significant contraction of C-C bonds. As a result, the hexagonal structure is less compressible than the flattened tube, which is a serious disadvantage for the reduction of van der Waals intertube repulsion. This is reflected in the value of the shortest intertube C-C distance, which is 2.9 Å for the hexagonal B, compared to a value of 3.3 Å for the flattened C, even though the RV for C is actually slightly smaller. It indicates much stronger van der Waals repulsion in B due to its structural inflexibility.

Another interesting indication of the stability of various structures is shown in Table I, which lists the relative energy of a single tube. For each structure, the atomic coordinates are taken directly from the corresponding structure in Fig. 1, and a single tube is then put in a box with a and b at 25 Å.

(6,6)
RV   0.730
Stress   12.5 GPa

(8,8)
RV   0.538
Stress   13.0 GPa
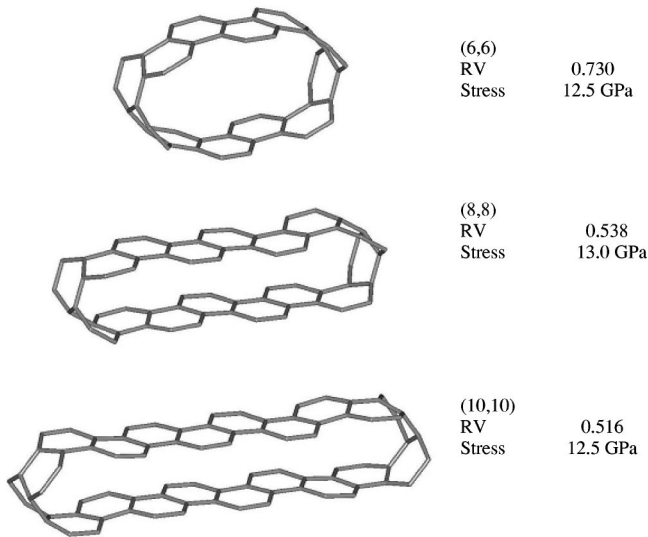
(10,10)
RV   0.516
Stress   12.5 GPa

FIG. 3. The flattened tube structures in a crystalline bundle of (6,6), (8,8), or (10,10) tubes at a lattice stress around 13 GPa. The structures of (8,8) and (10,10) tubes are similar to each other, with longer flat sections for the (10,10) tubes. The distance between the two flat graphene sections is around 3.8 Å for both the (8,8) and (10,10) structures at such high pressure, approaching the interlayer distance of 3.35 Å in graphite. The (6,6) structure is somewhat elliptical, due to its small diameter.

The calculated total energy for a flattened C tube is 0.6 eV lower than that for a hexagonal B tube. As there are two tubes in a unit cell for our model of a tube bundle, the tube structures contributes 1.2 eV for the decrease of 5.1 eV in total energy as the hexagonal B is transformed into the flattened C, while the other 3.9 eV can be attributed to the decrease in van der Waals repulsion.

B. Dependence on tube diameters

The slope of the stress versus RV curve shown in Figs. 1 and 2 indicates a trend that the tubes with smaller diameters are harder to compress. It can be accounted by two factors. First, the cap sections are localized and their sizes do not change significantly with tube diameters, while an increase in the tube diameter would elongate the flattened sections. The larger the flattened section, the more effective the conjugate π bonding, which in turn compensate the bond buckling in the cap sections. On the other hand, the flattening of

TABLE I. Relative energy of a single (10,10) carbon nanotube frozen at A–D as shown in Fig. 1. With the single tube in a 25 $\times$ 25 $\times$ 4.996-Å box, there is no van der Waals interactions between tubes in neighboring cells.

Tube structure as in Fig. 1	Relative energy (eV)
D	12.5
C	2.3
B	2.9
A	0.0

tubes with larger diameters results in a larger decrease in their volumes, and thus a larger reduction in the van der Waals repulsion. Thus, for tubes with large diameters, the flattened structure should be more advantageous over the hexagonal structure in terms of energy. And these considerations should not be effected by symmetry constraints.

However, in a recent DFT study on the compressed (10,10) and (12,12) bundles, Sluiter *et al.* argued that the deformation into hexagonal or elliptical sections upon pressure is driven by symmetry.[24] This was based on the observation of hexagonal section for the (12,12) bundle, and elliptical section for the (10,10) bundle, which was attributed to the fact that the (12,12) tubes were commensurate with the hexagonal symmetry of the lattice, while the (10,10) tubes were not. We would argue that the symmetry factor probably trapped the (12,12) in the hexagonal structure, which is a local minimum. Significantly, they observed the hexagonal structure for the (12,12) bundle up to a pressure of only 6 GPa. The same is true in our calculations. Only at pressure higher than 10 GPa, the structure optimization breaks out of the hexagonal structure B and locates the real minimum in C (Fig. 1).

It should also be noted that the tubes we studied have diameters around 10 Å or less, and their sections are circular at zero pressure. Upon compression, the section shape then changes first into elliptical and then flattened structure, while the metastable hexagonal section is only observed under high pressure due to the symmetry constraints of the lattice on our structure optimization. As discussed before, for bundles of larger tubes with diameter larger than 17 Å, the tube sections are hexagonal even at zero pressure.[13,34] At low pressure, they remain the minimum structure, while at high pressure, there may well be an energy barrier for the transformation from a hexagonal section to the more stable flattened section, which could trap the tubes in the hexagonal shape and should be an interesting subject for future studies.

C. Volume compressibility

By numerical fitting the data points in Fig. 1, the value of $\partial V/\partial P$ can be estimated and volume compressibility calculated by $\nu = -(1/V)(\partial V/\partial P)$, as listed in Table II. As the tube sections change from circular to elliptical and then to flattened shape upon compression, the compressibility actually increases. It is an interesting and somewhat counterintuitive trend: the tube becomes softer as pressure is increased. Overall the values of ν in Table I are very favorably compared with the compressibility of graphite at ~ 0.028 GPa^{-1}. The flattened structure C, with ν at 0.158 GPa^{-1}, is the most elastic. It responds to further compression with longer graphene sections, and shorter and more strained cap sections, which reduces the tube interiors, as in D. Such a fairly unusual structural response, with stress localized in the cap sections and taken up by the facile bond buckling, explains the extraordinary elasticity in carbon nanotubes. There are also limits to the compressibility, as seen in the region of $RV < 0.6$, with the resistance to pressure increasing significantly.

For structure D, the distance between the two graphene sections is ~ 3.8 Å, which can be compared with the graphite

TABLE II. Calculated volume compressibility for a crystalline bundle of (10,10) carbon nanotubes, from the curve shown in Fig. 1.

Reduced volume/ structure	RV region	Volume compressibility (GPa^{-1})
$RV = 1.0$ circular	$0.89 < RV < 1.00$	0.038
$RV = 0.89$ circular/ hexagonal	$0.80 < RV < 0.89$	0.012
$RV = 0.89$ elliptical	$0.80 < RV < 1.00$	0.089
$RV = 0.78$ flattened	$0.60 < RV < 0.78$	0.158
$RV = 0.60$ flattened	$0.50 < RV < 0.60$	0.015

interlayer distance of 3.35 Å. At such a distance, there may well be weakly intratube attractive interactions between the two graphene sections, similar to the interlayer interactions in graphite. Further compression is possible, but it will soon reach the stiff limit of van der Waals repulsion between the graphene sections, when the distance falls below 3.35 Å. Breaking down of the cap sections due to excessive bond buckling is also possible, especially for small tubes, by either the breaking of the carbon-carbon bond, or more likely, by the formation of sp^3 bonds forming intertube links. However, in our calculation, such chemical changes are not observed at a stress up to $\sim$20 GPa. More generally, an array of carbon nanotubes can be thought as an array of cylinders, albeit with molecular dimensions. The patten of compression and eventual collapse at the molecular level shall be very interesting comparison to that at the macroscopic level modeled by continuum mechanics.[35]

It has been demonstrated that the resistivity of carbon nanotube ropes is pressure dependent,[36] which is related to the pressure induced structural changes. With the large extent of structural deformation over an impressive range of pres-sure, as shown in our calculations, a bundle of CN's could be potentially used as electromechanical devices, such as gauges in a high-pressure environment.

In terms of chemical properties, the flat graphene sections should resemble graphite and be relatively inert. On the other hand, due to the stress localized in the cap sections and the large degree of bond buckling, the caps should be chemically active, which is enhanced by increasing pressure. It thus provides a pressure-dependent chemical environment, which is an interesting area for future investigation.

V. CONCLUSION

We have studied the deformation of the tube sections under high pressure for the crystalline bundle of (10,10), (8,8), and (6,6) single walled carbon nanotubes. The structures with hexagonal tube sections are a metastable state, due to the symmetry constraint of the triangular lattice. Such a section is too rigid to reduce the tube volumes and the intertube van der Waals repulsion. A flattened section is identified, which is consisted of two flat sections connected by two cap sections, similar to the shape of a 400-m track. With the stress localized on the cap sections, the bundle is stabilized by the more effective conjugate π bonding on the two flat sections, and by the significant reduction in tube volumes, and thus in the intertube van der Waals repulsion. It also provides a pressure dependent environment with the stressed cap sections being chemically more reactive than the flat sections.

*Corresponding authors.

[1] M. S. Dresselhaus, G. Dresselhaus, and P. C. Eklund, *Science of Fullerenes and Carbon Nanotubes* (Academic, New York, 1996).

[2] B. Vigolo, A. Penicaud, C. Coulon, C. Sauder, R. Pailler, C. Journet, P. Bernier, and P. Poulin, Science **290**, 1331 (2000); R. H. Baughman, *ibid.* **290**, 1310 (2000).

[3] M. M. J. Treacy, T. W. Ebbesen, and J. M. Gibson, Nature (London) **381**, 678 (1996).

[4] B. I. Yakobson, C. J. Brabec, and J. Bernholc, Phys. Rev. Lett. **76**, 2511 (1996).

[5] G. H. Gao, T. Çağin, and W. A. Goddard III, Nanotechnology **9**, 184 (1998).

[6] S. Iijima, C. Brabec, A. Maiti, and J. Bernholc, J. Chem. Phys. **104**, 2089 (1996).

[7] N. G. Chopra, L. X. Benedict, V. H. Crespi, M. L. Cohen, S. G. Louie, and A. Zettl, Nature (London) **377**, 135 (1995).

[8] R. S. Ruoff, J. Tersoff, D. C. Lorents, S. Subramoney, and B. Chan, Nature (London) **364**, 514 (1993).

[9] J. C. Charlier, X. Gonze, and J. P. Michenaud, Europhys. Lett. **29**, 43 (1995).

[10] H. W. Zhu, C. L. Xu, D. H. Wu, B. Q. Wei, R. Vajtai, and P. M. Ajayan, Science **296**, 884 (2002).

[11] A. Thess, R. Lee, P. Nikalaev, H. J. Dai, P. Petit, J. Robert, C. Xu, Y. H. Lee, S. G. Kim, A. G. Rinzler, D. T. Colbert, G. E. Scuseria, D. Tomanek, J. E. Fischer, and R. E. Smalley, Science **273**, 483 (1996).

[12] C. Journet, W. K. Maser, P. Bernier, A. Loiseau, M. L. de la Chapelle, S. Lefrant, P. Deniard, R. Lee, and J. E. Fischer, Nature (London) **388**, 756 (1997).

[13] J. Tersoff and R. S. Ruoff, Phys. Rev. Lett. **73**, 676 (1994).

[14] C. Q. Ru, Phys. Rev. B **62**, 10 405 (2000).

[15] S. A. Chesnokov, V. A. Nalimova, A. G. Rinzler, R. E. Smalley, and J. E. Fischer, Phys. Rev. Lett. **82**, 343 (1999).

[16] U. D. Venkateswaran, A. M. Rao, E. Richter, M. Menon, A. Rinzler, R. E. Smalley, and P. C. Eklund, Phys. Rev. B **59**, 10 928 (1999).

[17] M. J. Peters, L. E. McNeil, J. P. Lu, and D. Kahn, Phys. Rev. B **61**, 5939 (2000).

[18] P. V. Teredesai, A. K. Sood, D. V. S. Muthu, R. Sen, A. Govindaraj, and C. N. R. Rao, Chem. Phys. Lett. **319**, 296 (2000).

[19] U. D. Venkateswaran, E. A. Brandsen, U. Schlecht, A. M. Rao, E. Richter, I. Loa, K. Syassen, and P. C. Eklund, Phys. Status Solidi B **223**, 225 (2001).

[20] D. Khan and J. P. Lu, Phys. Rev. B **60**, 6535 (1999).

[21] J. Tang, L. C. Qin, T. Sasaki, M. Yudasaka, A. Matsushita, and S. Iijima, Phys. Rev. Lett. **85**, 1887 (2000).

[22] S. M. Sharma, S. Karmakar, S. K. Sikka, P. V. Teredesai, A. K. Sood, A. Govindaraj, and C. N. R. Rao, Phys. Rev. B **63**, 205417 (2001).

[23] S. Rols, I. N. Goncharenko, R. Almairac, J. L. Sauvajol, and I. Mirebeau, Phys. Rev. B **64**, 153401 (2001).

[24] M. H. F. Sluiter, V. Kumar, and Y. Kawazoe, Phys. Rev. B **65**, 161402 (2002).

[25] R. Car and M. Parrinello, Phys. Rev. Lett. **55**, 2471 (1985).

[26] M. L. Cohen, Phys. Rep. **110**, 293 (1984).

[27] D. Vanderbilt, Phys. Rev. B **41**, 7892 (1990).

[28] G. Kresse and J. Hafner, J. Phys.: Condens. Matter **6**, 8245 (1994).

[29] J. P. Perdew, in *Electronic Structure of Solids '91*, edited by P. Ziesche and H. Eschrig (Academie Verlag, Berlin, 1991), p. 11.

[30] G. Kresse and J. Furthmüller, Phys. Rev. B **54**, 11 169 (1996).

[31] G. Kresse and J. Hafner, Phys. Rev. B **47**, 558 (1993).

[32] G. Kresse and J. Furthmüller, Comput. Mater. Sci. **6**, 15 (1996).

[33] S. P. Chan, G. Chen, X. G. Gong, and Z. F. Liu, Phys. Rev. Lett. **87**, 205502 (2001).

[34] M. J. López, A. Rubio, J. A. Alonso, L. C. Qin, and S. Iijima, Phys. Rev. Lett. **86**, 3056 (2001).

[35] S. D. Papka and S. Kyriakides, Int. J. Solids Struct. **36**, 4397 (1999).

[36] R. Gaál, J. P. Salvetat, and L. Forró, Phys. Rev. B **61**, 7320 (2000).